INFECTION AND IMMUNITY, July 2008, p. 3001–3010 Vol. 76, No. 7
0019-9567/08/$08.00+0 doi:10.1128/IAI.00215-08

Initial Delay in the Immune Response to *Francisella tularensis* Is Followed by Hypercytokinemia Characteristic of Severe Sepsis and Correlating with Upregulation and Release of Damage-Associated Molecular Patterns▽

Chris A. Mares,[1] Sandra S. Ojeda,[1] Elizabeth G. Morris,[2] Qun Li,[2] and Judy M. Teale[1,2]*

Department of Microbiology and Immunology, The University of Texas Health Science Center at San Antonio, 7703 Floyd Curl Drive, San Antonio, Texas 78229,[1] and South Texas Center for Emerging Infectious Diseases and Department of Biology, The University of Texas at San Antonio, One UTSA Circle, San Antonio, Texas 78249[2]

Received 15 January 2008/Returned for modification 27 March 2008/Accepted 4 April 2008

"*Francisella tularensis* subsp. *novicida*" intranasal infection causes a rapid pneumonia in mice with mortality at 4 to 6 days with a low dose of bacteria (10^2 bacteria). The short time to death suggests that there is a failure of the innate immune response. As the neutrophil is often the first cell type to infiltrate sites of infection, we focused on the emigration of neutrophils in this infection, as well as cytokines involved in their recruitment. The results indicated that there was a significant delay in the influx of neutrophils into the bronchoalveolar lavage fluid of *F. tularensis* subsp. *novicida*-infected mice. The delay in neutrophil recruitment in *F. tularensis* subsp. *novicida*-infected mice correlated with a delay in the upregulation of multiple proinflammatory cytokines and chemokines, as well as a delay in caspase-1 activation. Strikingly, the initial delay in the upregulation of cytokines through 1 day postinfection was followed by profound upregulation of multiple cytokines and chemokines to levels consistent with hypercytokinemia described for severe sepsis. This finding was further supported by a bacteremia and the cellular relocalization and release of high-mobility group box-1 and S100A9, both of which are damage-associated molecular pattern molecules and are known to be mediators of severe sepsis.

Francisella tularensis is a gram-negative intracellular coccobacillus that causes tularemia, a life-threatening zoonotic infection of humans. The natural reservoir of this bacterium is not known for certain, but the host range is quite extensive as *F. tularensis* has been isolated from a wide array of both vertebrate and invertebrate hosts. Transmission can occur through many routes, and the course of disease depends on the route of infection (13, 17). Infection occurs through ingestion of contaminated water or food, via an arthropod vector, by direct contact through mucosa or broken skin, or through inhalation of bacteria. An infection can occur with as few as 10 organisms by the inhalation route, and disease resulting from this mode of infection can result in overwhelming sepsis that is associated with the highest rate of mortality (4, 20, 25, 48).

F. tularensis has been the subject of intense research as it is considered among the most probable agents to be used in a biological attack. The fact that a few organisms can cause overwhelming disease suggests that this organism is able to evade the innate immune response. Polymorphonuclear leukocytes (PMNs), one of the first cell types recruited to the area of infection, appear to provide some protection (11), although defects in neutrophil responses have also been described (30, 31, 41, 54). *Francisella* is found primarily in host macrophages, and it escapes from the phagosome and replicates in the cytosol (9, 22, 29, 55). Cytosolic bacteria are sensed intracellularly by the innate immune system's pattern recognition receptors, which often leads to activation of caspase-1 within a molecular complex called the inflammasome, and there are several types of inflammasomes (26, 40, 58). This can result in both host cell death and release of proinflammatory cytokines, including interleukin-1β (IL-1β) and IL-18 (24, 27, 37). It has recently been shown that in vitro *Francisella* is capable of inducing IL-1β processing with kinetics characteristic of an early inflammasome (21, 36).

This study was initiated to explore potential mechanisms by which *Francisella* evades the innate immune response in an intact animal. The kinetics of cytokine and chemokine expression during infection by *Francisella* and the kinetics of PMN recruitment to the foci of infection were determined first. The initial delay in expression of inflammatory cytokines was followed by widespread upregulation of multiple cytokines and chemokines resembling a cytokine storm, as described previously for infections associated with severe sepsis (60). Consistent with the late hypercytokinemia is a bacteremia and the relocalization of high-mobility group box-1 (HMGB-1), a prototype mediator of sepsis (62), as well as an increase in the level of S100A9, a potent endogenous immune mediator.

MATERIALS AND METHODS

Mice. Female C57BL/6 mice that were 6 to 8 weeks old and were obtained from the Charles River Laboratories (Frederick, MD) were used in all studies. Intranasal infection was performed by initially anesthetizing mice by intramus-

* Corresponding author. Mailing address: Department of Biology, The University of Texas at San Antonio, One UTSA Circle, San Antonio, TX 78249-1644. Phone: (210) 458-7024. Fax: (210) 458-7025. E-mail: judy.teale@utsa.edu.

▽ Published ahead of print on 14 April 2008.

cular injection of 100 μl of a ketamine-xylazine mixture (30 mg/ml ketamine and 4 mg/ml xylazine in phosphate-buffered saline [PBS]), followed by inoculation of 10 μl of a bacterial suspension in each nostril drop by drop (total volume, 20 μl), and allowing the mice to inhale the inoculum. Mock-infected animals received PBS, and samples were taken at the same time points as samples of their infected counterparts (6 h postinfection [hpi] and 1 and 3 days postinfection [dpi]). The results for mock-infected mice were averaged as they yielded virtually the same information regardless of the time that the mice were sacrificed. All the experimental procedures were in compliance with the guidelines of the institutional animal care and use committee.

Bacterial strains and culture media. "*Francisella tularensis* subsp. *novicida*" strain U112 and *F. tularensis* subsp. *tularensis* Schu S4 were obtained from Bernard Arulanandam (University of Texas at San Antonio) through Fran Nano (University of Victoria). *F. tularensis* subsp. *novicida* was grown in Trypticase soy agar or broth (Becton Dickinson) supplemented with 0.1% cysteine. *F. tularensis* subsp. *tularensis* Schu S4 was grown in Trypticase soy agar or broth supplemented with 0.1% cysteine, 0.1% Casamino Acids, 250 μg/ml sodium pyruvate, 250 μg/ml ferrous sulfate, and 250 μg/ml sodium metabisulfite. *F. tularensis* subsp. *novicida* was resuspended and then plated to determine the titer in the original aliquot. The desired dose was then calculated from the amount of bacteria that was determined for the original aliquot. A dose of 4.45×10^2 CFU/20 μl was used for intranasal infection as this dose has been observed to cause mortality for nearly all mice used in experiments in our lab within 4 to 6 days. The numbers of CFU inoculated were confirmed at the time of infection by plating on TSA plus cysteine.

Preparation of lung frozen sections. In order to harvest the lungs, we modified a previously described protocol to better suit our model (10). Mice were anesthetized at serial time points with a mixture of ketamine and xylazine as described above. The pericardium and trachea were exposed by dissection. An incision was made in the trachea, and a sterile flexible cannula attached to a 3-ml syringe was inserted. The lungs of mice were inflated slowly with 0.5 to 0.7 ml of a Tissue-Tek OCT compound (Sakura Finetek, Torrance, CA)–2 M sucrose (1:1, vol/vol) solution. The trachea was initially ligated with string after the lungs were inflated in order to maintain the OCT-sucrose solution in the lungs, and this was followed by individual ligation of the right and left bronchi. The inflated lungs were then removed, embedded in Tissue-Tek OCT compound, and stored at −80°C. Nine-micrometer sections of lungs were obtained by using a Shandon Cryotome SME (Thermo Electron Corporation, Pittsburg, PA). One in every five slides containing lung sections was fixed in formalin for 10 min at room temperature (RT) and stained with hematoxylin and eosin to examine lung pathology, as well as the degree of cellular infiltration. The remaining slides were air dried overnight and fixed in fresh acetone for 20 s at RT. Acetone-fixed sections were wrapped in aluminum foil and stored at −80°C or were processed immediately for immunofluorescence microscopy.

Bronchoalveolar lavage. At serial time points tracheotomies were performed after mice were anesthetized with a mixture of ketamine and xylazine; a sterile flexible cannula attached to a 3-ml syringe was inserted into the trachea. The lungs were lavaged with 0.5-ml aliquots of a lavage solution (1× PBS, 3 mM EDTA, 100 μM isoproterenol) until 3 ml had been used. The bronchoalveolar lavage fluid (BALF) was centrifuged at 1,300 rpm for 7 min, and the supernatant was stored at −80°C for subsequent cytokine and chemokine analysis, which was performed by using the Rodent Multi-Analyte Profile (Luminex) available from Rules Based Medicine (Austin, TX). The remaining cell pellet was resuspended in sterile PBS, and the concentration was adjusted to 1×10^5 cells/ml. Cytocentrifugation was performed at 1,000 rpm for 7 min, and this was followed by Diff-Quik staining (Dade Behring Inc., Newark, DE) for differential cell counting.

Antibodies. The antibodies used for this study included anti-IL-1β biotinylated mouse anti-mouse antibody (Endogen, Woburn, MA), anti-cleaved caspase-1 purified goat anti-mouse antibody (Santa Cruz Biotechnology, Santa Cruz, CA), anti-IL-18 (active form) purified rat anti-mouse antibody (MBL, Woburn, MA), anti-CXCL2 (MIP-2) purified goat anti-mouse antibody (R&D Systems, Minneapolis, MN), goat anti-S100A9 antibody (R&D Systems Minneapolis, MN), and anti-HMGB-1 (Abcam, Inc., Cambridge, MA) purified rabbit anti-mouse antibody. IL-1β was detected with streptavidin-rhodamine red X conjugate (Molecular Probes, Eugene, OR). IL-18 was detected with a rhodamine red X-conjugated AffiniPure anti-rat immunoglobulin G (IgG) (Jackson ImmunoResearch Laboratories, Inc., West Grove, PA). CXCL2 was detected with a rhodamine red X-conjugated AffiniPure anti-goat IgG (Jackson ImmunoResearch Laboratories, Inc., West Grove, PA). S100A9 was detected with Alexa 488-conjugated chicken anti-goat antibody (Jackson ImmunoResearch Laboratories, Inc., West Grove, PA.). Anti-HMGB-1 was detected with Alexa 488-conjugated chicken anti-rabbit IgG (Molecular Probes, Eugene, OR).

Immunofluorescence microscopy. Lung sections were thawed at RT for 30 min. Tissues were fixed at −20°C in acetone and then in 70% ethanol, and then they were hydrated in PBS. Immunofluorescence analysis was performed by blocking tissue sections and incubating them with one or two sets of primary and secondary antibodies. Nonspecific binding was avoided by blocking for 30 min at RT with serum from the same species from which the fluorochrome-conjugated antibodies used were derived. Tissue sections were incubated for 40 min with primary antibodies diluted in species-specific serum at concentrations that had previously been optimized. After incubation with specific antibodies, sections were washed seven times for 3 min each time. Secondary antibodies were incubated for 30 min at RT (when necessary). When double staining was performed, a second set of primary antibodies was incubated with the corresponding secondary antibody. Sections were then mounted with Fluorsave reagent (Calbiochem, La Jolla, CA) containing 0.3 μM 4′,6′-diamidino-2-phenylindole dilactate (DAPI) (Molecular Probes, Eugene, OR). Fluorescence was visualized with a Leica DMR epifluorescence microscope (Leica Microsystems, Wetzlar, Germany). Images were acquired using a cooled SPOT RT charge-coupled device camera (Diagnostic Instruments Inc., Sterling Heights, MI), and they were processed and analyzed using Adobe Photoshop 7.0 (Adobe, Mountain View, CA). The IPLab 3.7 imaging software (BD Biosciences, Rockville, MD) was used to quantify mean pixel intensity, as well as the percentage of the region of interest, defined as follows: (total area/area of region of interest) × 100. Data were collected from three different experiments ($n = 3$) using at least three independent areas of tissue for HMGB-1 and S100A9 staining. Results for these data are shown below for one representative experiment.

Cell culture infection. Murine macrophage-like cell line J774.A1 was grown on coverslips in cell monolayers (2×10^5 cells per well) and infected for 2 h with *F. tularensis* subsp. *tularensis* Schu S4 at a multiplicity of infection (MOI) of 50 in 24-well plates. The coverslips were harvested at various time points after infection and processed for immunofluorescence staining. Whole-cell extracts were also prepared in parallel wells and harvested at the same time points after infection, and they were subsequently used for Western blot analysis.

Determination of numbers of CFU in blood. Blood was collected from sacrificed mice that had previously been infected intranasally with 4.45×10^2 CFU/20 μl via cardiac puncture with heparin sodium salt as an anticoagulant. Blood was then serially diluted, and the dilutions were plated on TSA plates supplemented with cysteine. The plates were incubated at 37°C for 24 h, and the numbers of CFU were subsequently calculated.

Statistical analysis. A statistical analysis was performed using the Student *t* test (SigmaPlot 8.0). *P* values of <0.05 were considered significant.

RESULTS

Infiltration of neutrophils into lungs of intranasally infected mice. As neutrophils are among the first cell types recruited during an innate immune response, we examined infiltration of neutrophils into the lungs of mice infected with *F. tularensis* subsp. *novicida*. The percentage of neutrophils at 6 hpi in the BALF of *F. tularensis* subsp. *novicida*-infected animals was similar to that in mock-infected animals, and an increase was not observed until 1 dpi (Fig. 1A) ($P < 0.01$). The percentage of neutrophils remained relatively constant in *F. tularensis* subsp. *novicida*-infected animals through 3 dpi ($P < 0.005$). Furthermore, we also looked at the total number of neutrophils infiltrating into the BALF, and a substantial increase in the number of PMNs was observed at 1 dpi (Fig. 1B). The largest number of PMNs was observed at 3 dpi ($P < 0.05$). We concurrently checked the bacterial burden in the BALF at 6 hpi and 1 dpi and noted that bacteria were present at both early time points. At 6 hpi we detected $5.2 \times 10^1 \pm 2.0 \times 10^1$ CFU/ml, and at 1 dpi we detected $2.48 \times 10^5 \pm 1.3 \times 10^4$ CFU/ml. Although the *F. tularensis* subsp. *novicida* bacterial burden in the BALF was lower at 6 hpi, increasing the dose of *F. tularensis* subsp. *novicida* to 2×10^4 CFU/20 μl did not result in a change in the kinetics of neutrophil influx (data not shown).

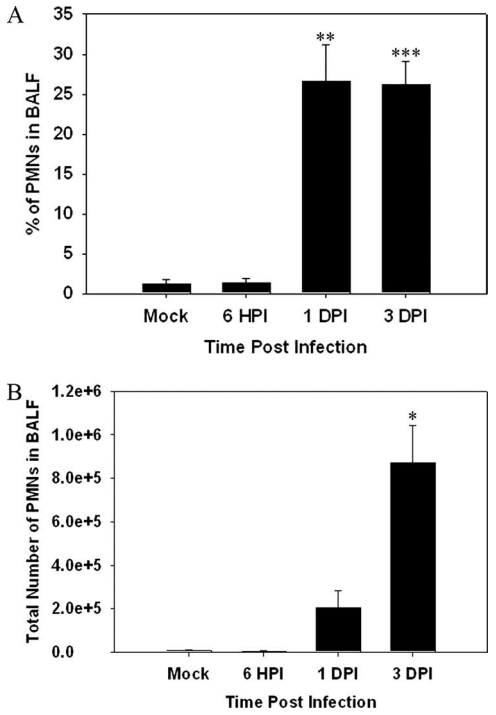

FIG. 1. Neutrophil infiltration into lungs of mice infected with *Francisella* is delayed. BALF was harvested and cytocentrifuged, and the resulting slides were stained with Diff-Quik to determine cell types. (A) Percentages of neutrophils in BALF obtained from mice ($n = 3$ for each group and each time point) infected with *Francisella* at 6 hpi and 1 and 3 dpi. (B) Total numbers of neutrophils entering the BALF calculated for the same time points. One asterisk, $P < 0.05$; two asterisks, $P < 0.01$; three asterisks, $P < 0.005$.

Delay of expression of chemokines important for neutrophil chemotaxis in BALF of infected mice. Given the delay in the kinetics of neutrophil accumulation in *F. tularensis* subsp. *novicida*-infected mice, we examined the timing of expression and levels of chemokines in BALF using Luminex technology, and we placed particular emphasis on the chemokines CXCL1 (Gro-α), CXCL2 (MIP-2), and CXCL6 (GCP-2) important for neutrophil migration and mobilization. All three of these chemokines were not upregulated until 3 dpi in the BALF of mice infected with *F. tularensis* subsp. *novicida* (Fig. 2A, B, and C) (for CXCL1, $P < 0.01$; for CXCL2, $P < 0.005$; and for CXCL6, $P < 0.005$). In addition, the concentration of granulocyte-macrophage colony-stimulating factor, a cytokine important for mobilization of neutrophils from the bone marrow (23), was also not significantly increased in the *F. tularensis* subsp. *novicida* infection model until 1 dpi ($P < 0.005$) and 3 dpi (Fig. 2D).

To substantiate these results, in situ immunofluorescence was used to analyze the expression of various chemokines and cytokines in infected lung tissue sections. Representative results for CXCL2 are shown in Fig. 2E. In mock-infected mice there was a relatively low level of expression in the lung parenchyma (Fig. 2E, panel E1), but there was constitutive expression in bronchial epithelial cells (Fig. 2E, panel E1). The same expression pattern for CXCL2 was observed at both 6 hpi and 1 dpi (Fig. 2E, panels E2 and E3). In contrast, in mice infected with *Francisella*, CXCL2 expression was highly upregulated in bronchial epithelial cells, as well as in the peribronchial infiltrates at 3 dpi (Fig. 2E, panel E4). A similar delay until 3 dpi was observed for increased expression of CXCL1 (data not shown) in *F. tularensis* subsp. *novicida*-infected mice.

Kinetics of inflammasome-related molecules in vivo. IL-1β and IL-18 are both considered indicators of inflammasome formation (39, 53). Recent evidence has suggested that the inflammasome may be involved in *Francisella* infections (21, 36, 63). Therefore, we compared the kinetics of these molecules in our infection model in vivo. In *Francisella*-infected animals the levels of IL-1β were found to be greater than the control levels only at 3 dpi (Fig. 3A) ($P < 0.001$). These results were corroborated by immunofluorescence staining, which revealed relatively low IL-1β expression in the lungs of *F. tularensis* subsp. *novicida*-infected animals through 1 dpi (Fig. 3C, panels C2 and C3) and an increase in expression at 3 dpi (Fig. 3C, panel C4).

The level of IL-18 was also not significantly elevated until 3 dpi in *F. tularensis* subsp. *novicida*-infected mice (Fig. 3B) ($P < 0.05$). The staining pattern for IL-18 also showed a delay in expression in the lungs of mice infected with *F. tularensis* subsp. *novicida* until 3 dpi (Fig. 3D, panels D2 and D4).

In order to exert its effects on IL-1β and IL-18, caspase-1 must be cleaved so that it becomes active. Using an antibody that recognizes cleaved caspase-1, we assessed the expression of active caspase-1 in vivo using immunofluorescence. We observed that cleaved caspase-1 staining did increase in the lungs of *Francisella*-infected mice until 3 dpi (Fig. 3E, panels E2 and E3).

Hypercytokinemia appears to follow an initial delay in cytokine expression. We noticed that in addition to the delay in chemokine expression, the peak concentrations of CXCL2, CXCL6, and CXCL1 in BALF of *F. tularensis* subsp. *novicida*-infected mice were significantly greater than those in mock-infected animals. A similar finding was obtained for IL-18 (Fig. 3). The levels and timing of expression of several additional cytokines in the BALF were also examined (Table 1). Similar to the findings for the cytokines described above, elevated expression of most of the cytokines was not detected until 3 dpi. In addition, the levels of several of the cytokines were 10- to 500-fold greater than the control levels. To determine if the increases were systemic, cytokine concentrations in sera were determined (Table 2). Serum levels of cytokines were generally not observed until 3 dpi, and the increases observed were striking in most cases. Suspecting sepsis, we examined the presence of *F. tularensis* subsp. *novicida* in the blood of infected animals by performing a CFU analysis (Table 3). The results indicate that there was a bacteremia along with the hypercytokinemia observed at 3 and 4 dpi.

Detection of HMGB-1 after infection with *Francisella*. The striking upregulation of multiple cytokines is consistent with what was recently reported for severe sepsis (34). As extracellular HMGB-1 is a potential prototype mediator of sepsis, its expression was examined in the lungs of mice infected with *F. tularensis* subsp. *novicida* (Fig. 4A, panels A1 to A4). In the lungs of mock-infected animals, HMGB-1 expression was largely restricted to an intracellular localization either in the nucleus or in the cytoplasm in the alveolar and bronchial ep-

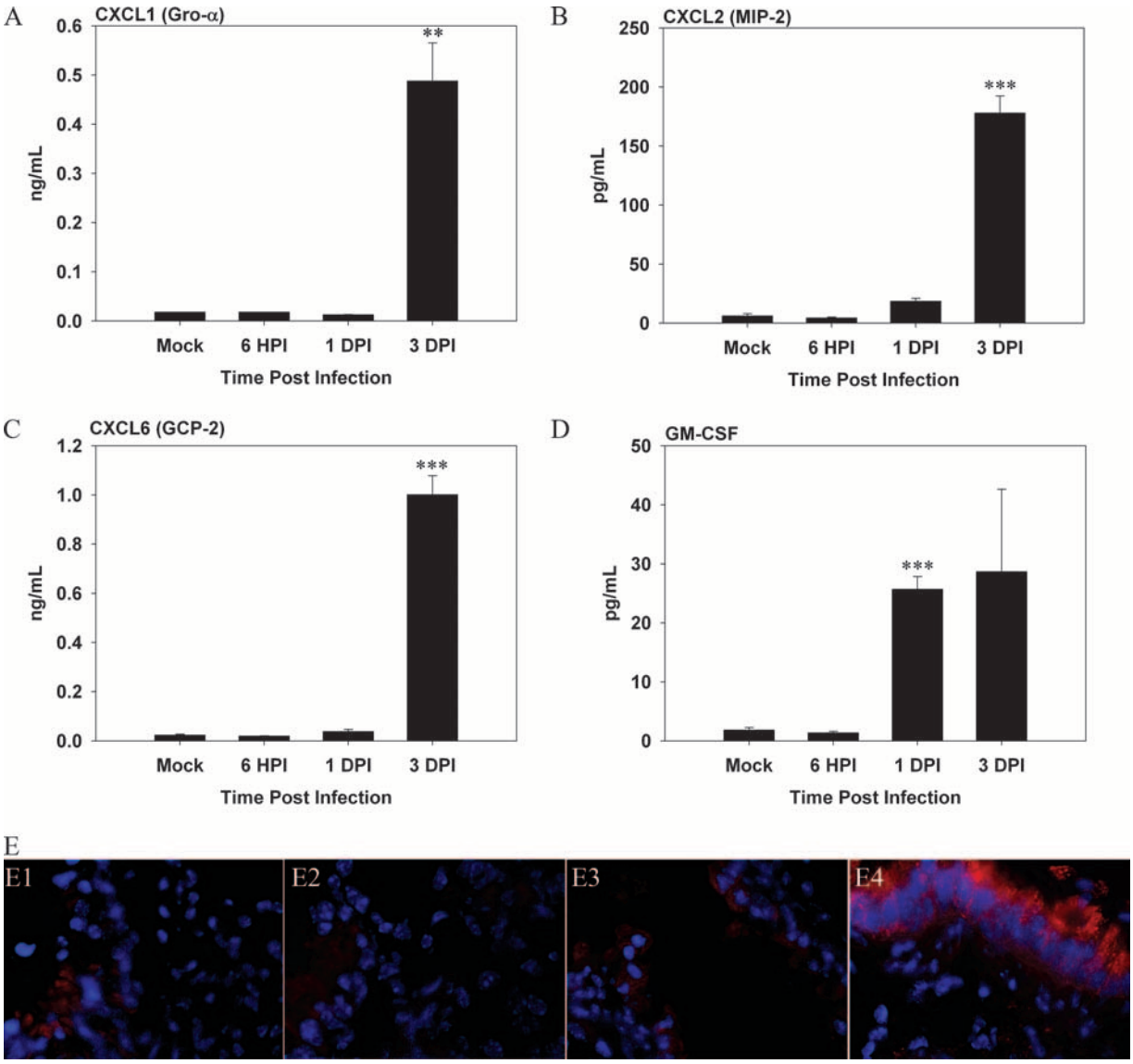

FIG. 2. Kinetics of cytokines important for neutrophil chemotaxis is delayed in BALF of mice infected with *Francisella*. (A to D) BALF was harvested from mice ($n = 3$ per time point) infected with *Francisella* at 6 hpi and 1 and 3 dpi. Concentrations of (A) CXCL1 (Gro-α), (B) CXCL2 (MIP-2), (C) CXCL6 (GCP-2), and (D) granulocyte-macrophage colony-stimulating factor (GM-CSF) were determined using Luminex assays. The data are the averages for three infected mice per time point. One asterisk, $P < 0.05$; two asterisks, $P < 0.01$; three asterisks, $P < 0.005$. (E) Lung sections prepared from infected animals at indicated time points were incubated with anti-CXCL2, followed by rhodamine red X-conjugated anti-goat IgG, and were analyzed by in situ immunofluorescence microscopy. Nuclei of cells (blue) were visualized by staining with DAPI. Panel E1 is a representative image for mock-infected mice, showing a constitutive level of CXCL2 present in the lungs, especially in the bronchioles. Mice were infected with *Francisella* for 6 h (panel E2), 1 day (panel E3), or 3 days (panel E4). Magnification for all panels, ×800.

ithelial cells (Fig. 4A, panel A1). Not much change was observed in the alveoli or bronchial epithelium at 6 hpi (Fig. 4A, panel A2). Modest amounts of HMGB-1 were detected in the lumen of blood vessels, as well as in some alveolar air sacs, at this early time point (unpublished results). Interestingly, HMGB-1 was found to be substantially upregulated as a result of infection, and importantly, much of it was localized outside cells by 1, 2, and 3 dpi (Fig. 4A, panels A3 and A4) (data not shown for 2 dpi). Figure 4D also shows that there was a significant increase in the percentage of the area positive for HMGB-1 expression with time postinfection ($P < 0.005$), as determined by an IPLab 3.7 software analysis of in situ immunofluorescence data. We also checked HMGB-1 in cells from the BALF (Fig. 4B, panels B1 to B4) and detected relocalization of HMGB-1 from the nucleus and/or cytoplasm to the cell membrane at both 6 hpi (Fig. 4B, panel B2) and 3 dpi (Fig. 4B, panel B4). The potential relocalization of HMGB-1 was also examined in J774 cells infected with *F. tularensis* subsp. *tularensis* Schu S4 (Fig. 4C, panels C1 to C4). In uninfected cells the expression of HMGB-1 was relatively low, and HMGB-1 was present mainly in the nucleus (Fig. 4C, panel C1). Increased expression was observed as early as 8 hpi (Fig. 4C, panel C2), and expression increased with time postinfection (Fig. 4C, panel C3), but

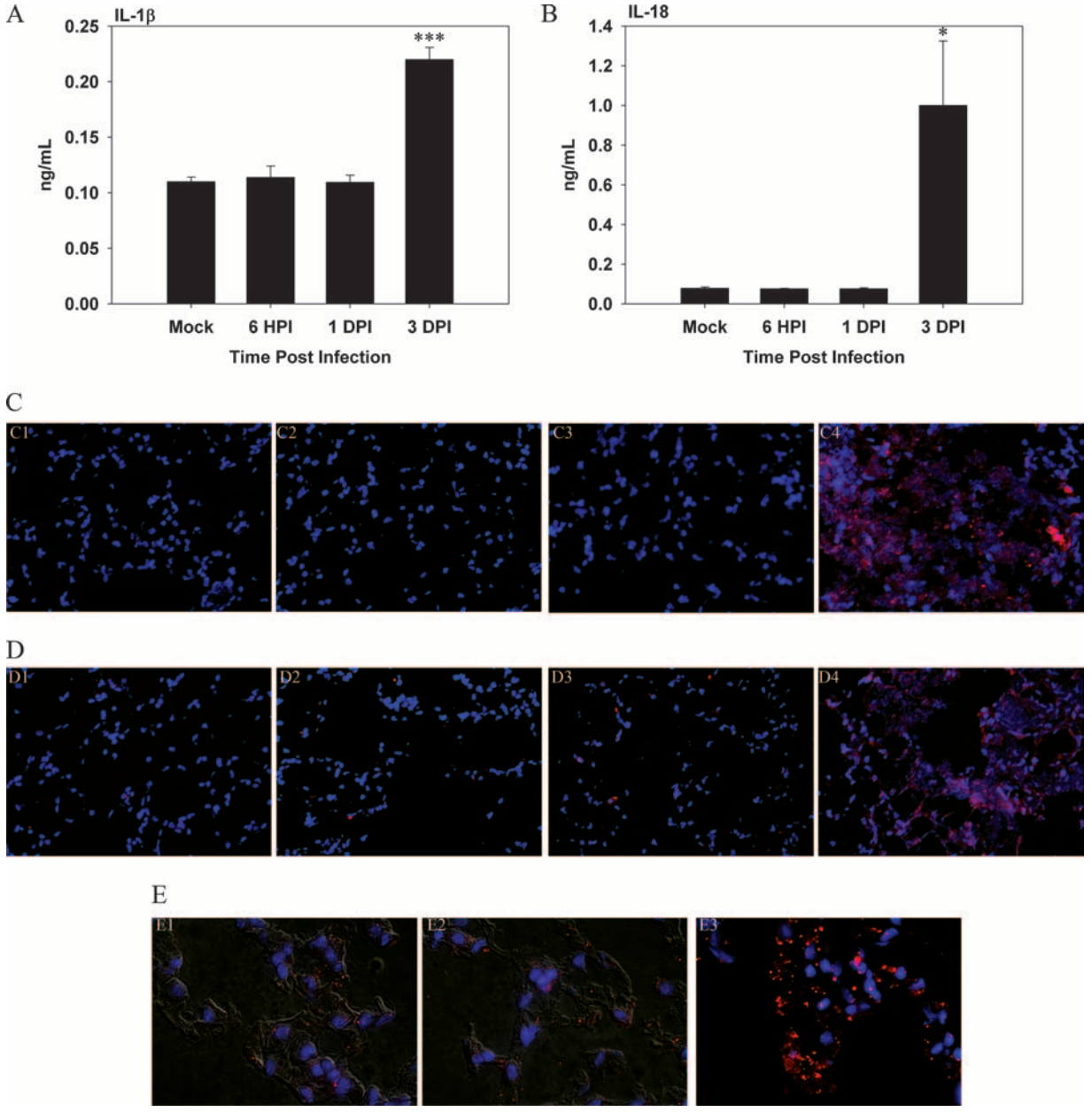

FIG. 3. Kinetics of inflammasome-associated cytokines is delayed in vivo in BALF of mice infected with *Francisella*. BALF was harvested from *Francisella*-infected mice, and levels of IL-1β and IL-18 were measured using Luminex assays. (A) IL-1β levels in BALF of mice ($n = 3$) infected with *Francisella* at the indicated time points. (B) Concentrations of IL-18 in BALF. One asterisk, $P < 0.05$; three asterisks, $P < 0.005$. (C) Immunofluorescence microscopy performed to visualize the expression of IL-1β in vivo. Streptavidin-rhodamine red X was used to visualize IL-1β, while DAPI was used to visualize nuclei. Panel C1 is an image of a mock-infected control. Panels C2, C3, and C4 are images of *F. tularensis* subsp. *novicida*-infected mice at 6 hpi and 1 and 3 dpi, respectively. Magnification, ×400. (D) Immunofluorescence microscopy performed to analyze the kinetics of IL-18 in vivo. Panel D1 is an image of a mock-infected control. Panels D2, D3, and D4 show IL-18 expression in mice infected with *F. tularensis* subsp. *novicida* at 1 and 3 dpi, respectively. Magnification, ×400. (E) Expression of active caspase-1. Panel E1 shows expression of active caspase-1 in vivo in a mock-infected lung. Panels E2 and E3 show active caspase-1 expression at 6 hpi and 3 dpi, respectively. Panels E1 and E2 show images merged with differential interference contrast images. Magnification, ×1,000.

the majority of extracellular HMGB-1 was observed at 72 hpi (Fig. 4C, panel C4). Finally, using Western blot analysis, we also determined that HMGB-1 expression from whole-cell extracts of J774 macrophages infected with Schu S4 (MOI, 50) increased with time postinfection (Fig. 4E). The greatest increases were detected at 24, 48, and 72 hpi. Similar increases in HMGB-1 expression were detected by Western blot analysis in whole-cell extracts of cells isolated from the BALF of mice infected with *F. tularensis* subsp. *novicida* (unpublished data).

Detection of S100A9 after infection with *Francisella*. We next investigated another recently described damage-associated

TABLE 1. Hypercytokinemia observed in BALF from mice infected with *F. tularensis* subsp. *novicida*

Mediator	Concn[a]				
	Control	6 hpi	1 dpi	3 dpi	4 dpi
IL-1α	35.1 ± 3.0	32.2 ± 1.9	38.5 ± 2.1	161 ± 27.8	151 ± 30.7
IL-6	3.5 ± 0.6	2.9 ± 0.5	10.1 ± 0.3	324 ± 106	447 ± 167
Gamma interferon	21.7 ± 6.3	15.1 ± 3.5	16.0 ± 1.8	161 ± 48.4	174 ± 60.2
Tumor necrosis factor alpha	32 ± 6	31 ± 3	34 ± 1	379 ± 65	507 ± 152
CXCL10	17.6 ± 3.0	20.5 ± 1.9	28.9 ± 1.2	4,993 ± 882	4,267 ± 1,020
CCL2	8.5 ±1.4	8.1 ± 1.9	10.3 ± 0.9	5,137 ± 1,455	7,533 ± 2,783
CCL7	10.8 ± 1.8	11.6 ± 2.1	18.2 ± 1.2	4,583 ± 803	6,460 ± 1,618
CCL12	<9.3	<9.3	<9.3	224 ± 33.5	271 ± 76.4
CCL22	15.9 ± 1.3	16.4 ± 1.4	20.7 ± 1.0	51.9 ± 3.9	35.2 ± 7.6
CCL11	13.7 ± 0.1	13.8 ± 0.8	13.8 ± 0.8	66.8 ± 11.3	151 ± 48.2
XCL1	28.7 ±7.4	21.6 ±3.8	20.7 ± 2.3	103 ±19.3	129 ± 30.7
Macrophage colony-stimulating factor[b]	0.02 ± 0.0	0.02 ± 0.0	0.03 ± 0.0	0.91 ± 0.2	1.1 ± 0.3
CCL3[b]	<0.04	<0.04	<0.04	0.19 ± 0.02	0.24 ± 0.09
CCL4	67.2 ± 11.9	49.1 ± 8.9	58.4 ± 9.9	917 ± 153	1,780 ± 812
CCL10[b]	0.13 ± 0.05	0.15 ± 0.02	0.18 ± 0.01	1.61 ± 0.33	2.63 ± 0.64
OSM[b]	0.05 ± 0.01	0.04 ± 0.01	0.04 ± 0.01	0.18 ± 0.02	0.19 ± 0.03
CCL5	<9.6	<9.6	<9.6	45.9 ± 3.8	43.8 ± 20.8
IL-10	576 ± 71.0	496 ± 13.9	482 ± 8.1	822 ± 47.6	998 ± 153
IL-11	11.9 ± 2.6	9.9 ± 2.3	10.3 ± 1.3	25.5 ± 3.1	28.0 ± 3.3

[a] The concentrations of various immune mediators in the BALF from mice infected with *F. tularensis* subsp. *novicida* were determined by Luminex assays and are expressed in pg/ml unless indicated otherwise.
[b] The concentrations are expressed in ng/ml. All data for 3 dpi and most data for 4 dpi are significantly different ($P < 0.05$ to $P < 0.005$) than the control data.

molecular pattern molecule (DAMP) designated S100A9. Initially, we performed immunofluorescence microscopy to determine the localization of the protein in both mock- and *F. tularensis* subsp. *novicida*-infected animals. In mock-infected animals S100A9 was evident in cells widely interspersed throughout the lung (Fig. 5A, panel A1). Relatively little change was observed in this pattern at both 6 hpi and 1 dpi (Fig. 5A, panels A2 and A3). However, a substantial increase in the expression of S100A9 was observed at 3 dpi, and S100A9 seemed to be associated with lesions as well as present throughout the lung parenchyma. Figure 5B shows the percentage of area positive for S100A9 calculated from immunofluorescence microscopy data. However, the percentage of the area of tissue expressing S100A9 was almost 10-fold greater and in fact was significantly increased by 3 dpi compared with the mock infection levels ($P < 0.05$). Figure 5C shows the results of a representative experiment which showed that there was an increase in expression of S100A9 with time postinfection in the lung homogenates of mice infected with *F. tularensis* subsp. *novicida*.

TABLE 2. Hypercytokinemia is observed at the systemic level in mice infected with *F. tularensis* subsp. *novicida*

Mediator	Concn[a]				
	Control	6 hpi	1 dpi	3 dpi	4 dpi
Gamma interferon	<68	<68	<68	4,130 ± 1,656	1,184 ± 476
IL-6	<14	<14	<14	10,197 ± 6,145	13,662 ± 5,821
IL-18[b]	0.83	1.3	1.2	22.8 ± 4.2	41.3 ± 11.3
CXCL2	<7.2	<7.2	14.1	2,182 ± 999	7,666 ± 2,566
CCL7	156	147	142	9,737 ± 1,062	8,946 ± 1,689
CXCL10	<40	45	<40	20,765 ± 2,632	20,465 ± 2,932
CCL2	43	49	64	10,559 ± 1,628	6,053 ± 3,158
CXCL1[b]	<0.17	<0.17	<0.17	13.5 ± 3.5	34.3 ± 13.5
XCL1	<85	<85	<85	723 ± 83.5	897 ± 159
CCL12	<46	<46	<46	2,840 ± 892	4,857 ± 748
CCL4	<78	<78	<78	4,127 ± 1,417	6,450 ± 2,255
CCL10[b]	5.9	10.5	9.8	128 ± 45.9	186 ± 66.5
CCL19[b]	0.07	0.07	0.08	0.43 ± 0.09	0.63 ± 0.22
OSM[b]	<0.13	<0.13	<0.13	0.90 ± 0.04	1.04 ± 0.24
CCL5	<48	<48	<48	103 ± 19.6	206 ± 54.8
IL-4	<74	<74	<74	173 ± 29.8	209 ± 43.9
IL-10	109	137	140	5,380 ± 968	8,973 ± 2,199
IL-11	<87	<87	<87	341 ± 64	459 ± 9.3

[a] The systemic concentrations of cytokines and chemokines in the serum of mock-infected animals and animals infected with *F. tularensis* subsp. *novicida* at 6 hpi and 1, 3, and 4 dpi were determined using Luminex assays and are expressed in pg/ml unless indicated otherwise. The values are averages for measurements obtained for the control and early infection time points for biological duplicates. The values for 3 and 4 dpi were derived from the averages of biological triplicates.
[b] The values are expressed in ng/ml. The data for 3 and 4 dpi are significantly different ($P < 0.05$ to $P < 0.005$) than the control data for 6 hpi and 1 dpi.

TABLE 3. *F. tularensis* subsp. *novicida* establishes a bacteremia in blood

Time	Concn of bacteria (CFU/ml)
6 hpi	ND[a]
1 dpi	73 ± 64
3 dpi	$3.68 \times 10^5 \pm 1.60 \times 10^5$
4 dpi	$3.27 \times 10^6 \pm 7.49 \times 10^5$

[a] ND, not detected.

DISCUSSION

F. tularensis is a highly virulent organism, and the infectious dose required to cause fulminate disease is relatively low. This fact, combined with the development of *F. tularensis* as a bioweapon by various governments, has led to its designation as a potential biowarfare threat and thus inclusion on the CDC's Category A list (16, 42). *F. tularensis* subsp. *novicida* is similarly virulent in mice, particularly by the pulmonary route of infection, providing an important model system (4, 20, 25, 49). The

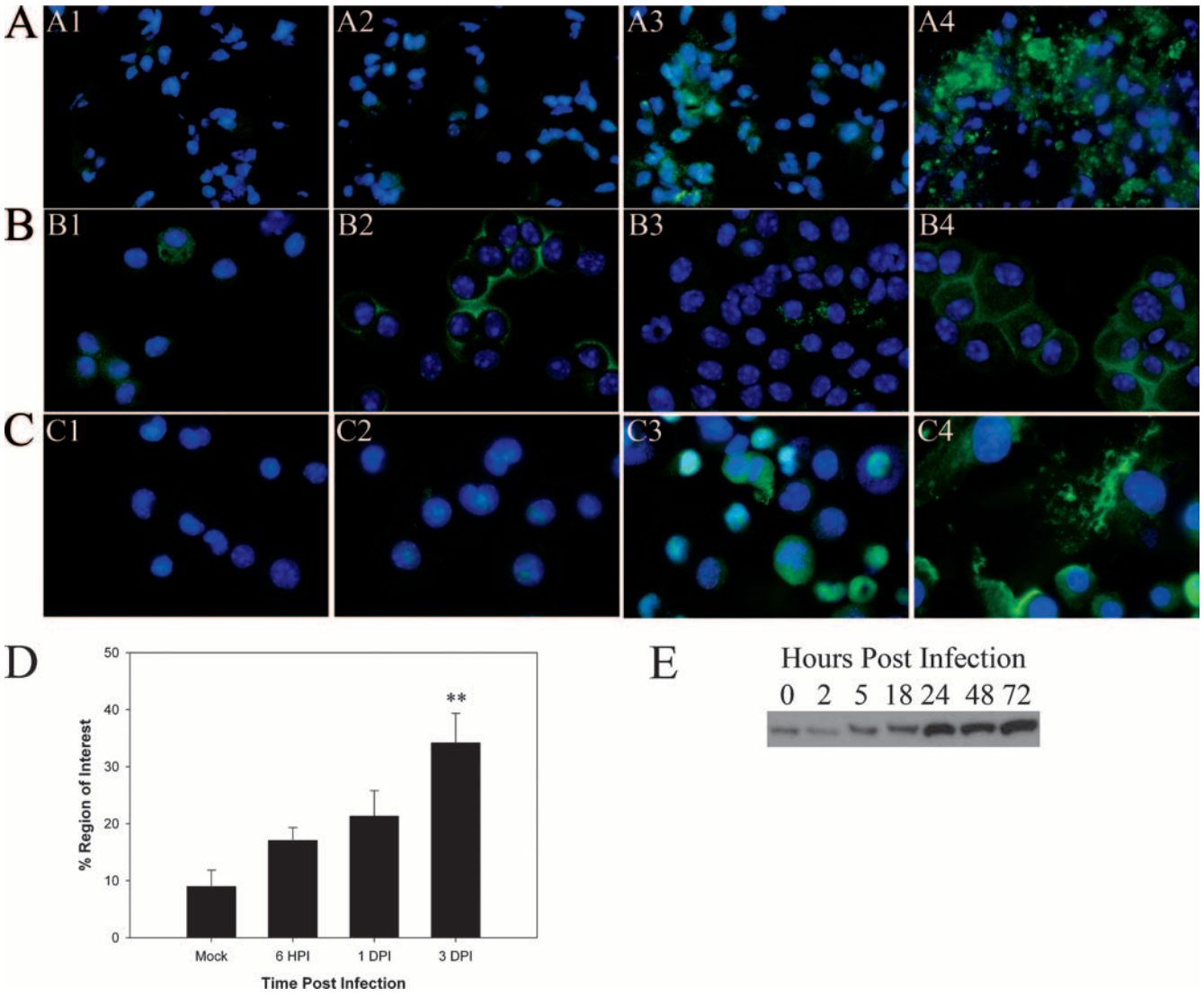

FIG. 4. HMGB-1 is released from cells infected with *Francisella* both in vivo and in vitro. Immunofluorescence microscopy was performed to determine the localization of HMGB-1 in the lungs of infected mice and in BALF cells, as well as in infected J774 cells. HMGB-1 was visualized with Alexa 488 (green), while DAPI was used to observe the nuclei. Magnification for panels A1 to A4 and B1 to B4, ×800X; magnification for panels C1 to C4, ×1,000. (A) Images of similar areas in the lung (lung parenchyma and alveolar epithelium). Panel A1 is an image for the lung of a representative mock-infected mouse, while panels A2, A3, and A4 are images for mice infected with *F. tularensis* subsp. *novicida* at 6 hpi and 1 and 3 dpi, respectively. Panel A4 shows HMGB-1 expression in a lesion in the lung at 3 dpi. (B) HMGB-1 expression in cells isolated from the BALF. Panel B1 is an image for cells harvested from a mock-infected animal, while panels B2, B3, and B4 are images for cells harvested at 6 hpi and 1 and 3 dpi, respectively. (C) Representative micrographs of J774 cells infected with *F. tularensis* subsp. *tularensis* Schu S4 at an MOI of 50 at 0, 8, 24, and 72 hpi (panels C1 to C4, respectively). (D) Percentage of the region of interest positive for HMGB-1 in multiple tissue sections as determined by using IPLabs 3.7. Two asterisks, $P < 0.01$. (E) Representative Western blot for two independent experiments probed for the presence of HMGB-1 using equivalent amounts of whole-cell extracts of J774 cells infected with Schu S4 at an MOI of 50 at the following time points: 0 (mock infection), 2, 5, 18, 24, 48, and 72 hpi.

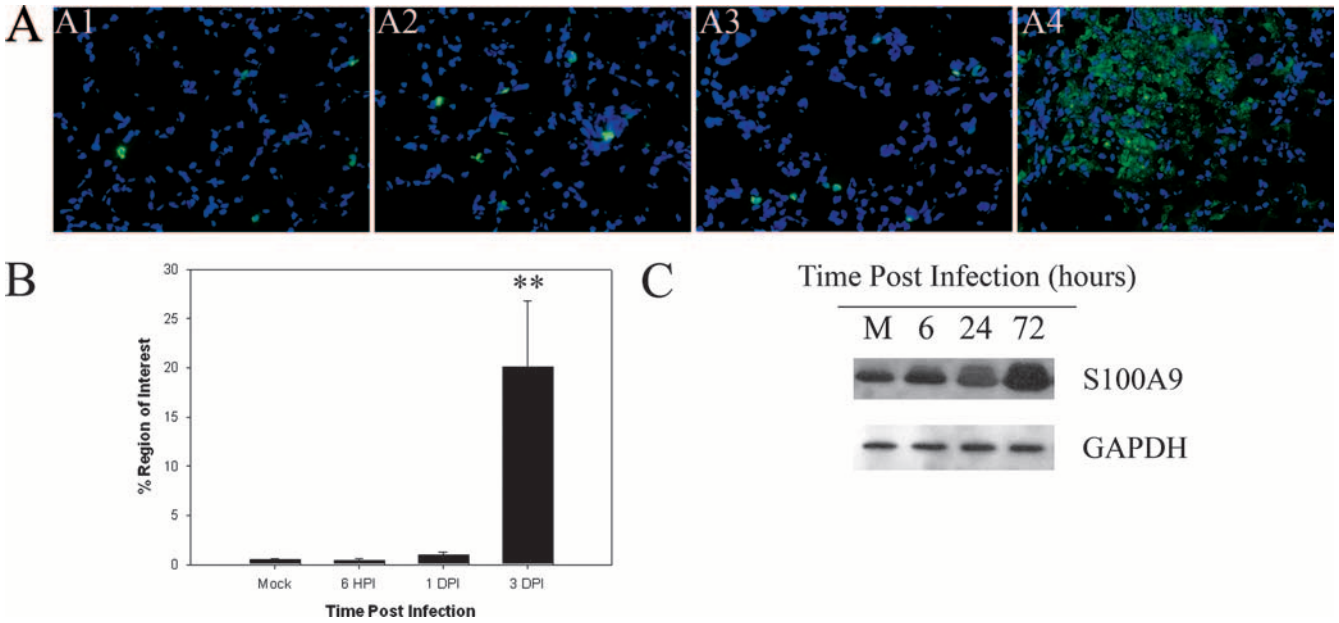

FIG. 5. S100A9 expression is increased in the lungs of mice infected with *F. tularensis* subsp. *novicida*. (A) S100A9 expression assessed using immunofluorescence microscopy with lung sections from mice infected with *F. tularensis* subsp. *novicida*. Panel A1 shows S100A9 expression in mock-treated animals. Panels A2, A3, and A4 show S100A9 expression in *F. tularensis* subsp. *novicida*-infected lungs at 6 hpi and 1 and 3 dpi, respectively. All images are images of similar areas of the lung (lung parenchyma and alveolar epithelium). Magnification for all panels, ×400. (B) Percentage of the region of interest expressing S100A9 obtained from in situ immunofluorescence data for the lungs of mice infected with *F. tularensis* subsp. *novicida* using IPLabs 3.7 software. Two asterisks, $P < 0.01$. (C) Western blot demonstrating expression of S100A9 in lung homogenates obtained from mock-infected animals (lane M), as well as animals infected for 6, 24, and 72 hpi. The position of glyceraldehyde-3-phosphate dehydrogenase (GAPDH) is shown as a loading control for the assay. The blot is a representative Western blot for two independent experiments.

goal of our study was to better understand the host response in vivo to this pathogen. Initially, the kinetics of cells infiltrating into the BALF were examined. We found that the influx of neutrophils was delayed in mice infected with *F. tularensis* subsp. *novicida*. It is worth noting that we observed a similar defect in the ability of neutrophils to infiltrate into the BALF when we used a higher dose, 2×10^4 CFU/20 μl. We then tested cytokines important for neutrophil chemotaxis and mobilization, many of which have not been analyzed for tularemia previously. Particular attention was paid to the ELR^+ CXC chemokines, which are critical chemoattractants for neutrophils (8, 33, 35). The expression of these chemokines was found to be delayed in lungs of *F. tularensis* subsp. *novicida*-infected animals. However, the delay observed was not limited to ELR^+ CXC chemokines but applied to multiple proinflammatory cytokines and chemokines. Reminiscent of this, a delay in the upregulation of several immunity-related genes in *F. tularensis*-infected animals has been reported (2, 3). Although the mediator responsible for some influx of neutrophils at 1 dpi is unclear, the sheer number of proinflammatory cytokines still at the baseline level of expression at 1 dpi compared with data for other pulmonary infections indicates that there is a widespread delay in the immune response in *Francisella*-infected animals. For instance, we have also performed extensive studies with another respiratory pathogen, *Klebsiella pneumoniae*, and have examined many of the same parameters in this infection model that were examined in the *F. tularensis* subsp. *novicida* infection model. The most striking difference between the two infection models was the rapid response associated with *K. pneumoniae* with regard to the PMN influx into the BALF, as well as the rapid induction of expression of cytokines. The PMN response elicited by *K. pneumoniae* was vigorous and easily detected by 6 hpi. Lawlor et al. and Bubeck et al. have also reported that there is an early and vigorous inflammatory response in the lungs of mice infected with *Klebsiella* (7, 28). Similarly, in our studies with *Klebsiella*, the levels of many cytokines, including those important for neutrophil chemotaxis, were elevated by 6 hpi in *K. pneumoniae*-infected mice.

The virulence of intracellular organisms is largely associated with their ability to remain sequestered from many extracellular immune mediators, such as antibodies, complement, and other host proteases (57). However, intracellular pattern recognition receptors have been identified that make up part of the inflammasome, a multimolecular complex that results in cleavage of caspase-1, a cysteine protease involved in inflammation and cell death (14, 38, 39, 45, 59). Activation of the inflammasome results in processing and release of active IL-1β and IL-18 and is thought to be critical for immune defense against intracellular pathogens and other danger signals. Recently, it has been shown that infection of macrophages and dendritic cells in vitro with *Francisella* results in the release of IL-1β (21, 36) and IL-18, indicating that an inflammasome that involves ASC and caspase-1 may have a role (36). This release occurs within 6 h. In vivo, it has been reported that IL-1β processing can occur within a similar time frame (6 to 12 h) in mice infected with *Legionella pneumophila* (56). Similarly, mice infected with *Staphylococcus aureus* also produce IL-1β within 6 hpi (43). Results obtained here also indicate that IL-1β and

IL-18 release occurred as soon as 6 hpi in the case of *K. pneumoniae*-infected animals (data not shown). However, an increase in the IL-1β and IL-18 levels in mice infected with *F. tularensis* subsp. *novicida* was not detected until 3 dpi. Therefore, in addition to many other immune mediators, inflammasome activation appears to be delayed in vivo in mice infected with *F. tularensis* subsp. *novicida*.

The development of hypercytokinemia at both the local and systemic levels in infected mice is consistent with the cytokine profile of severe sepsis reported by Ulloa and Tracey (60). Also consistent with sepsis is the presence of *F. tularensis* subsp. *novicida* in the blood. Similarly, bacteremia has been reported in tularemia (17), and Forestal et al. have shown that both LVS and Schu S4 have an extracellular phase in mice and can be found in the blood (19). Aberrant upregulation of proinflammatory cytokines has been observed in H5N1 influenza and *Burkholderia* infections, as well as acute pancreatitis (12, 34, 47, 64). The three cytokines that are most diagnostic for sepsis are CXCL10 (IP-10), IL-6, and CXCL2 (MIP-2/IL-8) (6, 44, 50), and these cytokines have been shown to be systemically upregulated >500 to 1,000-fold in *F. tularensis* subsp. *novicida*-infected mice at 3 to 4 dpi, when animals are near death. Also relevant are the systemic increases in IL-10 and IL-4 expression, as sepsis leads to a shift in Th2 responses (6, 51). The observation that hypercytokinemia is coupled with the widespread cell death (unpublished data) most likely due to necrosis, apoptosis, and potentially pyroptosis has led us to hypothesize that DAMPs shed by dead or dying host cells or released by activated immune cells may have a substantial role in initiating and sustaining a hyperinflammatory environment that is lethal to the host. It is likely that the cytokine storm is a major contributor to the overt pathology and mortality associated with respiratory *Francisella* infections, and one of the DAMPs involved may be HMGB-1 (46). HMGB-1 is an abundant protein that can be found in the nucleus and cytoplasm of many cell types (5, 15). Recent studies have characterized the proinflammatory activity of HMGB-1 in experimental models of sepsis in which HMGB-1 is released from cells (1, 32, 60, 65). Our data indicate that the localization of HMGB-1 throughout the course of infection is altered and, more importantly, that its extracellular localization can be observed both in vitro and in vivo.

We also decided to look at another DAMP in order to further highlight the important role that these endogenous immune mediators may play in the pathogenesis of tularemia. We focused on S100A9. S100A9 is one of the most abundant proteins that is found in the cytoplasm of neutrophils and monocytes (52). Like HMGB-1, S100A9 has a dual role as both a protein important for cellular homeostasis and a potential mediator of an inflammatory response (18). S100A9 has also recently been described as an important endogenous activator that may promote lethality in septic shock (61), and its upregulation at the mRNA level has been described in a murine model using Schu S4 infections (2). Our studies have shown that the expression of S100A9 increases with time postinfection and is localized to inflamed sites within the *F. tularensis* subsp. *novicida*-infected lung in vivo. Furthermore, additional studies confirmed that neither the dramatic increase in S100A9 expression nor the drastic relocalization of HMGB-1 was evident in the lungs of *K. pneumoniae*-infected mice (data not shown). Our current experiments are focused on elucidating the contributions of HMGB-1 and S100A9, as well as other DAMPs, to the pathogenesis of tularemia.

We further speculate that *Francisella* has a replicative niche early in the infection process that is sustained by delayed expression of multiple proinflammatory cytokines. This latent period allows the bacterium to replicate relatively unchecked. The resulting high bacterial loads lead to tissue destruction and the release of endogenous danger signals, such as HMGB-1, S100A9, and possibly other DAMPs. This leads to dysregulation of cytokines and chemokines related to sepsis, which ultimately leads to multiple organ failure and the fatal outcome associated with pneumonic tularemia.

ACKNOWLEDGMENTS

This study was supported by awards 1P01A10157986, NS35974, and AI 59703 from the National Institutes of Health. C.A.M. was also supported by departmental training grant T32AI7271 from the NIH.

REFERENCES

1. **Abraham, E., J. Arcaroli, A. Carmody, H. Wang, and K. J. Tracey.** 2000. HMG-1 as a mediator of acute lung inflammation. J. Immunol. **165:**2950–2954.
2. **Andersson, H., B. Hartmanova, R. Kuolee, P. Ryden, W. Conlan, W. Chen, and A. Sjostedt.** 2006. Transcriptional profiling of host responses in mouse lungs following aerosol infection with type A Francisella tularensis. J. Med. Microbiol. **55:**263–271.
3. **Andersson, H., B. Hartmanova, P. Ryden, L. Noppa, L. Naslund, and A. Sjostedt.** 2006. A microarray analysis of the murine macrophage response to infection with Francisella tularensis LVS. J. Med. Microbiol. **55:**1023–1033.
4. **Balagopal, A., A. S. MacFarlane, N. Mohapatra, S. Soni, J. S. Gunn, and L. S. Schlesinger.** 2006. Characterization of the receptor-ligand pathways important for entry and survival of *Francisella tularensis* in human macrophages. Infect. Immun. **74:**5114–5125.
5. **Bell, C. W., W. Jiang, C. F. Reich III, and D. S. Pisetsky.** 2006. The extracellular release of HMGB1 during apoptotic cell death. Am. J. Physiol. Cell Physiol. **291:**C1318–C1325.
6. **Bone, R. C., C. J. Grodzin, and R. A. Balk.** 1997. Sepsis: a new hypothesis for pathogenesis of the disease process. Chest **112:**235–243.
7. **Bubeck, S. S., A. M. Cantwell, and P. H. Dube.** 2007. Delayed inflammatory response to primary pneumonic plague occurs in both outbred and inbred mice. Infect. Immun. **75:**697–705.
8. **Charo, I. F., and R. M. Ransohoff.** 2006. The many roles of chemokines and chemokine receptors in inflammation. N. Engl. J. Med. **354:**610–621.
9. **Clemens, D. L., B. Y. Lee, and M. A. Horwitz.** 2004. Virulent and avirulent strains of *Francisella tularensis* prevent acidification and maturation of their phagosomes and escape into the cytoplasm in human macrophages. Infect. Immun. **72:**3204–3217.
10. **Coalson, J. J.** 1983. A simple method of lung perfusion fixation. Anat. Rec. **205:**233–238.
11. **Conlan, J. W., R. KuoLee, H. Shen, and A. Webb.** 2002. Different host defences are required to protect mice from primary systemic vs pulmonary infection with the facultative intracellular bacterial pathogen, Francisella tularensis LVS. Microb. Pathog. **32:**127–134.
12. **de Jong, M. D., C. P. Simmons, T. T. Thanh, V. M. Hien, G. J. Smith, T. N. Chau, D. M. Hoang, N. V. Chau, T. H. Khanh, V. C. Dong, P. T. Qui, B. V. Cam, Q. Ha do, Y. Guan, J. S. Peiris, N. T. Chinh, T. T. Hien, and J. Farrar.** 2006. Fatal outcome of human influenza A (H5N1) is associated with high viral load and hypercytokinemia. Nat. Med. **12:**1203–1207.
13. **Dennis, D. T., T. V. Inglesby, D. A. Henderson, J. G. Bartlett, M. S. Ascher, E. Eitzen, A. D. Fine, A. M. Friedlander, J. Hauer, M. Layton, S. R. Lillibridge, J. E. McDade, M. T. Osterholm, T. O'Toole, G. Parker, T. M. Perl, P. K. Russell, and K. Tonat.** 2001. Tularemia as a biological weapon: medical and public health management. JAMA **285:**2763–2773.
14. **Dinarello, C. A.** 2006. Interleukin 1 and interleukin 18 as mediators of inflammation and the aging process. Am. J. Clin. Nutr. **83:**447S–455S.
15. **Dumitriu, I. E., P. Baruah, A. A. Manfredi, M. E. Bianchi, and P. Rovere-Querini.** 2005. HMGB1: guiding immunity from within. Trends Immunol. **26:**381–387.
16. **Elkins, K. L., S. C. Cowley, and C. M. Bosio.** 2007. Innate and adaptive immunity to Francisella. Ann. N. Y. Acad. Sci. **1105:**284–324.
17. **Ellis, J., P. C. Oyston, M. Green, and R. W. Titball.** 2002. Tularemia. Clin. Microbiol. Rev. **15:**631–646.
18. **Foell, D., H. Wittkowski, T. Vogl, and J. Roth.** 2007. S100 proteins expressed in phagocytes: a novel group of damage-associated molecular pattern molecules. J. Leukoc. Biol. **81:**28–37.

19. **Forestal, C. A., M. Malik, S. V. Catlett, A. G. Savitt, J. L. Benach, T. J. Sellati, and M. B. Furie.** 2007. Francisella tularensis has a significant extracellular phase in infected mice. J. Infect. Dis. **196:**134–137.
20. **Gallagher, L. A., E. Ramage, M. A. Jacobs, R. Kaul, M. Brittnacher, and C. Manoil.** 2007. A comprehensive transposon mutant library of Francisella novicida, a bioweapon surrogate. Proc. Natl. Acad. Sci. USA **104:**1009–1014.
21. **Gavrilin, M. A., I. J. Bouakl, N. L. Knatz, M. D. Duncan, M. W. Hall, J. S. Gunn, and M. D. Wewers.** 2006. Internalization and phagosome escape required for Francisella to induce human monocyte IL-1beta processing and release. Proc. Natl. Acad. Sci. USA **103:**141–146.
22. **Golovliov, I., V. Baranov, Z. Krocova, H. Kovarova, and A. Sjostedt.** 2003. An attenuated strain of the facultative intracellular bacterium *Francisella tularensis* can escape the phagosome of monocytic cells. Infect. Immun. **71:**5940–5950.
23. **Hamilton, J. A., and G. P. Anderson.** 2004. GM-CSF Biology. Growth Factors **22:**225–231.
24. **Kanneganti, T. D., N. Ozoren, M. Body-Malapel, A. Amer, J. H. Park, L. Franchi, J. Whitfield, W. Barchet, M. Colonna, P. Vandenabeele, J. Bertin, A. Coyle, E. P. Grant, S. Akira, and G. Nunez.** 2006. Bacterial RNA and small antiviral compounds activate caspase-1 through cryopyrin/Nalp3. Nature **440:**233–236.
25. **Kieffer, T. L., S. Cowley, F. E. Nano, and K. L. Elkins.** 2003. Francisella novicida LPS has greater immunobiological activity in mice than F. tularensis LPS, and contributes to F. novicida murine pathogenesis. Microbes Infect. **5:**397–403.
26. **Lamkanfi, M., T. D. Kanneganti, L. Franchi, and G. Nunez.** 2007. Caspase-1 inflammasomes in infection and inflammation. J. Leukoc. Biol. **82:**220–225.
27. **Lara-Tejero, M., F. S. Sutterwala, Y. Ogura, E. P. Grant, J. Bertin, A. J. Coyle, R. A. Flavell, and J. E. Galan.** 2006. Role of the caspase-1 inflammasome in Salmonella typhimurium pathogenesis. J. Exp. Med. **203:**1407–1412.
28. **Lawlor, M. S., J. Hsu, P. D. Rick, and V. L. Miller.** 2005. Identification of Klebsiella pneumoniae virulence determinants using an intranasal infection model. Mol. Microbiol. **58:**1054–1073.
29. **Lindgren, H., I. Golovliov, V. Baranov, R. K. Ernst, M. Telepnev, and A. Sjostedt.** 2004. Factors affecting the escape of Francisella tularensis from the phagolysosome. J. Med. Microbiol. **53:**953–958.
30. **Lindgren, H., S. Stenmark, W. Chen, A. Tarnvik, and A. Sjostedt.** 2004. Distinct roles of reactive nitrogen and oxygen species to control infection with the facultative intracellular bacterium *Francisella tularensis*. Infect. Immun. **72:**7172–7182.
31. **Lofgren, S., A. Tarnvik, M. Thore, and J. Carlsson.** 1984. A wild and an attenuated strain of *Francisella tularensis* differ in susceptibility to hypochlorous acid: a possible explanation of their different handling by polymorphonuclear leukocytes. Infect. Immun. **43:**730–734.
32. **Lotze, M. T., and K. J. Tracey.** 2005. High-mobility group box 1 protein (HMGB1): nuclear weapon in the immune arsenal. Nat Rev. Immunol. **5:**331–342.
33. **Luster, A. D.** 1998. Chemokines—chemotactic cytokines that mediate inflammation. N. Engl. J. Med. **338:**436–445.
34. **Makhija, R., and A. N. Kingsnorth.** 2002. Cytokine storm in acute pancreatitis. J. Hepatobiliary Pancreat. Surg. **9:**401–410.
35. **Mantovani, A., R. Bonecchi, and M. Locati.** 2006. Tuning inflammation and immunity by chemokine sequestration: decoys and more. Nat. Rev. Immunol. **6:**907–918.
36. **Mariathasan, S., D. S. Weiss, V. M. Dixit, and D. M. Monack.** 2005. Innate immunity against Francisella tularensis is dependent on the ASC/caspase-1 axis. J. Exp. Med. **202:**1043–1049.
37. **Martinon, F., L. Agostini, E. Meylan, and J. Tschopp.** 2004. Identification of bacterial muramyl dipeptide as activator of the NALP3/cryopyrin inflammasome. Curr. Biol. **14:**1929–1934.
38. **Martinon, F., K. Burns, and J. Tschopp.** 2002. The inflammasome: a molecular platform triggering activation of inflammatory caspases and processing of proIL-beta. Mol. Cell **10:**417–426.
39. **Martinon, F., and J. Tschopp.** 2004. Inflammatory caspases: linking an intracellular innate immune system to autoinflammatory diseases. Cell **117:**561–574.
40. **Mayor, A., F. Martinon, T. De Smedt, V. Petrilli, and J. Tschopp.** 2007. A crucial function of SGT1 and HSP90 in inflammasome activity links mammalian and plant innate immune responses. Nat. Immunol. **8:**497–503.
41. **McCaffrey, R. L., and L. A. Allen.** 2006. Francisella tularensis LVS evades killing by human neutrophils via inhibition of the respiratory burst and phagosome escape. J. Leukoc. Biol. **80:**1224–1230.
42. **McLendon, M. K., M. A. Apicella, and L. A. Allen.** 2006. Francisella tularensis: taxonomy, genetics, and immunopathogenesis of a potential agent of biowarfare. Annu. Rev. Microbiol. **60:**167–185.
43. **Miller, L. S., R. M. O'Connell, M. A. Gutierrez, E. M. Pietras, A. Shahangian, C. E. Gross, A. Thirumala, A. L. Cheung, G. Cheng, and R. L. Modlin.** 2006. MyD88 mediates neutrophil recruitment initiated by IL-1R but not TLR2 activation in immunity against Staphylococcus aureus. Immunity **24:**79–91.
44. **Ng, P. C., K. Li, K. M. Chui, T. F. Leung, R. P. Wong, W. C. Chu, E. Wong, and T. F. Fok.** 2007. IP-10 is an early diagnostic marker for identification of late-onset bacterial infection in preterm infants. Pediatr. Res. **61:**93–98.
45. **Ogura, Y., F. S. Sutterwala, and R. A. Flavell.** 2006. The inflammasome: first line of the immune response to cell stress. Cell **126:**659–662.
46. **Oppenheim, J. J., and D. Yang.** 2005. Alarmins: chemotactic activators of immune responses. Curr. Opin. Immunol. **17:**359–365.
47. **Osterholm, M. T.** 2005. Preparing for the next pandemic. N. Engl. J. Med. **352:**1839–1842.
48. **Oyston, P. C., A. Sjostedt, and R. W. Titball.** 2004. Tularaemia: bioterrorism defence renews interest in Francisella tularensis. Nat. Rev. Microbiol. **2:**967–978.
49. **Pammit, M. A., V. N. Budhavarapu, E. K. Raulie, K. E. Klose, J. M. Teale, and B. P. Arulanandam.** 2004. Intranasal interleukin-12 treatment promotes antimicrobial clearance and survival in pulmonary *Francisella tularensis* subsp. *novicida* infection. Antimicrob. Agents Chemother. **48:**4513–4519.
50. **Plant, L., H. Wan, and A. B. Jonsson.** 2006. MyD88-dependent signaling affects the development of meningococcal sepsis by nonlipooligosaccharide ligands. Infect. Immun. **74:**3538–3546.
51. **Rice, T. W., and G. R. Bernard.** 2005. Therapeutic intervention and targets for sepsis. Annu. Rev. Med. **56:**225–248.
52. **Roth, J., T. Vogl, C. Sorg, and C. Sunderkotter.** 2003. Phagocyte-specific S100 proteins: a novel group of proinflammatory molecules. Trends Immunol. **24:**155–158.
53. **Rowe, S. J., L. Allen, V. C. Ridger, P. G. Hellewell, and M. K. Whyte.** 2002. Caspase-1-deficient mice have delayed neutrophil apoptosis and a prolonged inflammatory response to lipopolysaccharide-induced acute lung injury. J. Immunol. **169:**6401–6407.
54. **Sandstrom, G., S. Lofgren, and A. Tarnvik.** 1988. A capsule-deficient mutant of *Francisella tularensis* LVS exhibits enhanced sensitivity to killing by serum but diminished sensitivity to killing by polymorphonuclear leukocytes. Infect. Immun. **56:**1194–1202.
55. **Santic, M., M. Molmeret, K. E. Klose, S. Jones, and Y. A. Kwaik.** 2005. The Francisella tularensis pathogenicity island protein IglC and its regulator MglA are essential for modulating phagosome biogenesis and subsequent bacterial escape into the cytoplasm. Cell. Microbiol. **7:**969–979.
56. **Shinozawa, Y., T. Matsumoto, K. Uchida, S. Tsujimoto, Y. Iwakura, and K. Yamaguchi.** 2002. Role of interferon-gamma in inflammatory responses in murine respiratory infection with Legionella pneumophila. J. Med. Microbiol. **51:**225–230.
57. **Sjostedt, A.** 2006. Intracellular survival mechanisms of Francisella tularensis, a stealth pathogen. Microbes Infect. **8:**561–567.
58. **Sutterwala, F. S., Y. Ogura, and R. A. Flavell.** 2007. The inflammasome in pathogen recognition and inflammation. J. Leukoc. Biol. **82:**259–264.
59. **Tschopp, J., F. Martinon, and K. Burns.** 2003. NALPs: a novel protein family involved in inflammation. Nat. Rev. Mol. Cell Biol. **4:**95–104.
60. **Ulloa, L., and K. J. Tracey.** 2005. The "cytokine profile": a code for sepsis. Trends Mol. Med. **11:**56–63.
61. **Vogl, T., K. Tenbrock, S. Ludwig, N. Leukert, C. Ehrhardt, M. A. van Zoelen, W. Nacken, D. Foell, T. van der Poll, C. Sorg, and J. Roth.** 2007. Mrp8 and Mrp14 are endogenous activators of Toll-like receptor 4, promoting lethal, endotoxin-induced shock. Nat. Med. **13:**1042–1049.
62. **Wang, H., O. Bloom, M. Zhang, J. M. Vishnubhakat, M. Ombrellino, J. Che, A. Frazier, H. Yang, S. Ivanova, L. Borovikova, K. R. Manogue, E. Faist, E. Abraham, J. Andersson, U. Andersson, P. E. Molina, N. N. Abumrad, A. Sama, and K. J. Tracey.** 1999. HMG-1 as a late mediator of endotoxin lethality in mice. Science **285:**248–251.
63. **Weiss, D. S., T. Henry, and D. M. Monack.** 2007. Francisella tularensis: activation of the inflammasome. Ann. N. Y. Acad. Sci. **1105:**219–237.
64. **Wiersinga, W. J., M. C. Dessing, P. A. Kager, A. C. Cheng, D. Limmathurotsakul, N. P. Day, A. M. Dondorp, T. van der Poll, and S. J. Peacock.** 2007. High-throughput mRNA profiling characterizes the expression of inflammatory molecules in sepsis caused by *Burkholderia pseudomallei*. Infect. Immun. **75:**3074–3079.
65. **Yang, H., H. Wang, C. J. Czura, and K. J. Tracey.** 2005. The cytokine activity of HMGB1. J. Leukoc. Biol. **78:**1–8.

Editor: A. J. Bäumler